Chapter 10
Use of Combined Biogeochemical Model Approaches and Empirical Data to Assess Critical Loads of Nitrogen

Mark E. Fenn, Charles T. Driscoll, Qingtao Zhou, Leela E. Rao, Thomas Meixner, Edith B. Allen, Fengming Yuan and Timothy J. Sullivan

10.1 Introduction

Humans have perturbed the global nitrogen (N) cycle, in relative terms, to a greater degree than the much more widely recognized effects of man's activities on global carbon (C) cycling (Smil 2001). Because of widespread effects of N on the environment and on sensitive ecosystems, critical loads (CLs) of N are being increasingly used for quantifying and mapping the ecological and environmental effects of N (Hettelingh et al. 2008; Pardo et al. 2011). Critical loads are generally determined from observations or from models of varying degrees of complexity, from simple steady state to process-based dynamic models. Nitrogen CLs can be determined for aquatic and terrestrial ecosystems, both for acidification and eutrophication (N as a nutrient) effects.

M. E. Fenn (✉)
USDA Forest Service, Pacific Southwest Research Station, Riverside, CA, USA
e-mail: mfenn@fs.fed.us

C. T. Driscoll · Q. Zhou
Department of Civil and Environmental Engineering, Syracuse University, Syracuse, NY, USA

L. E. Rao
Department of Environmental Science and Center for Conservation Biology,
University of California, Riverside, CA, USA

T. Meixner
Department of Hydrology and Water Resources, University of Arizona, Tucson, AZ, USA

E. B. Allen
Department of Botany and Plant Sciences and Center for Conservation Biology,
University of California, Riverside, CA, USA

F. Yuan
Environmental Sciences Division, Oak Ridge National Laboratory, Oak Ridge, TN, USA

T. J. Sullivan
E&S Environmental Chemistry, Corvallis, OR, USA

W. de Vries et al. (eds.), *Critical Loads and Dynamic Risk Assessments*,
Environmental Pollution 25, DOI 10.1007/978-94-017-9508-1_10

A major strength of empirical CLs is that they are based on chemical or biological response data under real-world conditions. A limitation of the empirical approach is that results may only be applied with confidence to sites with highly similar biotic and environmental conditions. Empirical CLs are important, however, for validating CL values determined with models. Advantages of simulation approaches are that ecosystem responses to alternative scenarios can be tested. These might include changes in atmospheric deposition, disturbance or climatic conditions, and responses to silvicultural treatments, grazing, fire, and other disturbances (Gimeno et al. 2009). Simulation modelling allows temporal aspects of ecosystem response in relation to CLs and CL exceedances to be evaluated, including evaluation of historical and future conditions.

Biogeochemical models such as PnET-BGC, DayCent, MAGIC, and ForSAFE-VEG have been used to simulate biogeochemical ecosystem responses to factors such as changes in air pollution, climate change, and disturbance. These models can also be applied towards estimating CLs. Such applications are described in the following sections. Empirical CLs for NO_3^- leaching were determined based on NO_3^- concentrations in streams or lakes located across N deposition gradients. The lowest N deposition at which NO_3^- leaching begins to increase above that observed at low pollution sites was taken as the empirical NO_3^- leaching CL. Nitrogen fertilization treatments were used to develop empirical N CLs for plant community changes or for increased biomass and fuel accumulation and fire risk from the growth of invasive annual grass species in desert scrub habitats.

In this chapter, we emphasize the combined approach of calculating CLs from biogeochemical simulation models in conjunction with empirical analyses. This combined approach has been applied previously to mixed conifer forests in California (Fenn et al. 2008). Herein, N CLs are based on empirical and simulated nitrate (NO_3^-) concentrations in streamwater, acid neutralizing capacity (ANC) in lakes and streamwater, changes in lake diatom assemblages or alpine vegetation communities, and fuel accumulation resulting from growth of invasive grasses in arid ecosystems. In this chapter, case studies of the combined simulation and empirical N CL approaches are described for four ecosystems including mixed conifer forests and the combination of desert scrub and pinyon-juniper woodlands in California, alpine catchments of the Rocky Mountains in Colorado and lakes in the Adirondack Mountains in New York.

10.2 California Mixed Conifer Forests

Overstory species composition in mixed conifer forests of California varies depending on elevation and site conditions, but is typically characterized by dense mixed-age stands of pine (*Pinus* spp.) and often fir (*Abies* spp.) and incense cedar (*Calocedrus decurrens* (Torr.), Florin.) in addition to broadleaved species, typically oaks (*Quercus* spp.). The climate is Mediterranean, characterized by cool wet winters and hot and dry conditions during summer. Mixed conifer forests over much of the Transverse Ranges in southern California and in the south-western Sierra Nevada

Mountains are exposed to elevated concentrations of ozone (O_3) and atmospheric N deposition from urban and agricultural emissions sources.

10.2.1 Methodologies for Empirical and Model-based CLs for Nitrate Leaching and N Trace Gas Loss

The empirical threshold for NO_3^- leaching is based on the relationship between throughfall N deposition and an empirically derived clean-site threshold value for streamwater NO_3^-. The threshold was derived by comparing temporal profiles of streamwater NO_3^- concentrations in relatively pristine low N deposition catchments against profiles for catchments receiving varying levels of chronic N deposition inputs. Based on 28 streams from relatively low pollution catchments in southern California (Fenn and Poth 1999; Riggan et al. 1985), we determined that peak NO_3^- concentrations in runoff rarely exceed 0.2 mg NO_3-N l^{-1} (14.3 µmol l^{-1}). This concentration corresponds with those reported for relatively unpolluted streams in Sweden (De Vries et al. 2007). Thus, 14.3 µmol was selected as the critical threshold value for identifying catchments that are beginning to exhibit symptoms of N excess or N saturation. The empirical N CL for NO_3^- leaching is thus the N deposition input at which this critical threshold NO_3^- concentration is exceeded (Fenn et al. 2008).

The N deposition input leading to NO_3^- leaching was determined by linear regression of streamwater NO_3^- and throughfall N deposition data collected during winter high flow events from 11 sites in the San Bernardino and southern Sierra Nevada Mountains, encompassing a broad range of annual N deposition inputs (5.7–71.1 kg $ha^{-1}yr^{-1}$).

The DayCent biogeochemistry model version 4.5 was used to simulate historical N saturation symptoms such as N trace gas emissions from soil and NO_3^- leaching and to estimate the N deposition threshold for such losses. DayCent (Del Grosso et al. 2000; Parton et al. 1998, 2001) is the daily time step version of the CENTURY model (Parton et al. 1993). It simulates the biogeochemical processes of C, N, phosphorus (P), and sulfur (S) associated with soil organic matter in multiple ecosystem types. One feature of DayCent important to this study is the improved N cycling algorithms, including the simulation of N_2O, NO, and N_2 emissions resulting from nitrification and denitrification. DayCent was parameterized for a high (Camp Paivika, CP) and low (Barton Flats, BF) deposition site in the San Bernardino Mountains located 70 km east of Los Angeles, California. See Fenn et al. (2008) for further details of model parameterization.

In conducting model runs to estimate the CL for NO_3^- leaching, N deposition was increased from an assumed background level of 0.1 kg N $ha^{-1}yr^{-1}$–3 kg N $ha^{-1}yr^{-1}$ in 1930 and increased linearly to 10 kg N $ha^{-1}yr^{-1}$ by 1940. In 1940, N deposition was set at 19 different levels for each site ranging from 10 to 80 kg N $ha^{-1}yr^{-1}$ and maintained at these levels for simulations lasting for 120 years more in order to simulate dose/responses to increasing N deposition. Annual N deposition was set to vary randomly by $<10\%$. Based on simulated occurrences of peak streamwater

NO_3^- concentrations above the clean site threshold of 0.2 mg l^{-1}, we determined the N deposition rate at which CL exceedance would occur at the model sites. We included a stipulation that the critical NO_3^- leachate concentration must be exceeded at least once every 10 years on average to consider the threshold exceeded. Spurious NO_3^- exceedances that occur rarely due to extreme climatic events for example, do not indicate a catchment above the CL by our definition (Fenn et al. 2008).

10.2.2 Empirical and Model-based CLs for Mixed Conifer Forests in California

Measurements of peak NO_3^- concentrations at the 11 stream sampling sites used to estimate the empirical CL ranged from 0.07 to 107 µeq l^{-1}. Based on the linear regression (r^2 0.98) of streamwater NO_3^- vs. throughfall N deposition, the N deposition at which the critical threshold NO_3^- concentration (14.3 µeq l^{-1}) occurs is 17 kg N $ha^{-1}yr^{-1}$. This can be considered as the empirical threshold for NO_3^- leaching at these sites (95% confidence interval: 15–19 kg N $ha^{-1}yr^{-1}$).

The estimated N deposition thresholds (i.e., the CL) for NO_3^- leaching based on simulated NO_3^- concentrations in seepage water were 17 and 30 kg N $ha^{-1}yr^{-1}$ at CP and BF (Fig. 10.1a, b). This is based on N deposition occurring over a range of values for 30–60 years and with at least one occurrence per decade on average of a peak streamwater NO_3^- value over the 0.2 mg l^{-1} threshold. The simulated N deposition CL for NO_3^- leaching at CP (17 kg N $ha^{-1}yr^{-1}$) was equal to the empirical throughfall CL. Increasing the time period of elevated N deposition resulted in lower CL values. Reducing precipitation by 40% at CP increased the estimated CL from 17 to 20 kg N $ha^{-1}yr^{-1}$ (Fig. 10.1c). An approximate doubling of the precipitation at the much drier BF site (using CP precipitation levels) decreased the simulated CL from 30 to 7 kg N $ha^{-1}yr^{-1}$ over a 30–60 year deposition time frame (Fig. 10.1d). The simulated CL at BF increased to 16 kg $ha^{-1}yr^{-1}$ with doubled precipitation and a time frame of less than 30 years (Fig. 10.1d). The much lower simulated CL at BF compared to CP when precipitation values from CP were used is presumably due to the lower plant and microbial biomass and thus lower N demand and retention capacity at BF. Thus more N is available in soil with potential to be leached or emitted as trace gases.

We do not have sufficient field data on trace gas emissions to establish an empirical CL to protect against unacceptably high trace gas emissions. However, this CL can be estimated from the DayCent simulations. At the N deposition level equal to the empirical CL for NO_3^- leaching (17 kg N $ha^{-1}yr^{-1}$), simulated mean annual gaseous losses of N (including NO, N_2O and N_2) were ca. 1.8 kg N $ha^{-1}yr^{-1}$ at CP. If we set the acceptable gaseous N loss at 2 kg N $ha^{-1}yr^{-1}$, then the simulated CLs for trace gas loss are 20 and 10 kg N $ha^{-1}yr^{-1}$ at CP and BF, respectively (Fig. 10.1e, f). At CP and BF the percent of N deposition re-emitted as N trace gases in the year 2000 according to DayCent was 20 and 22% respectively. These results agree with European studies demonstrating that temperate forests show increased NO and N_2O fluxes when throughfall N deposition was greater than 15 kg $ha^{-1}yr^{-1}$ and that

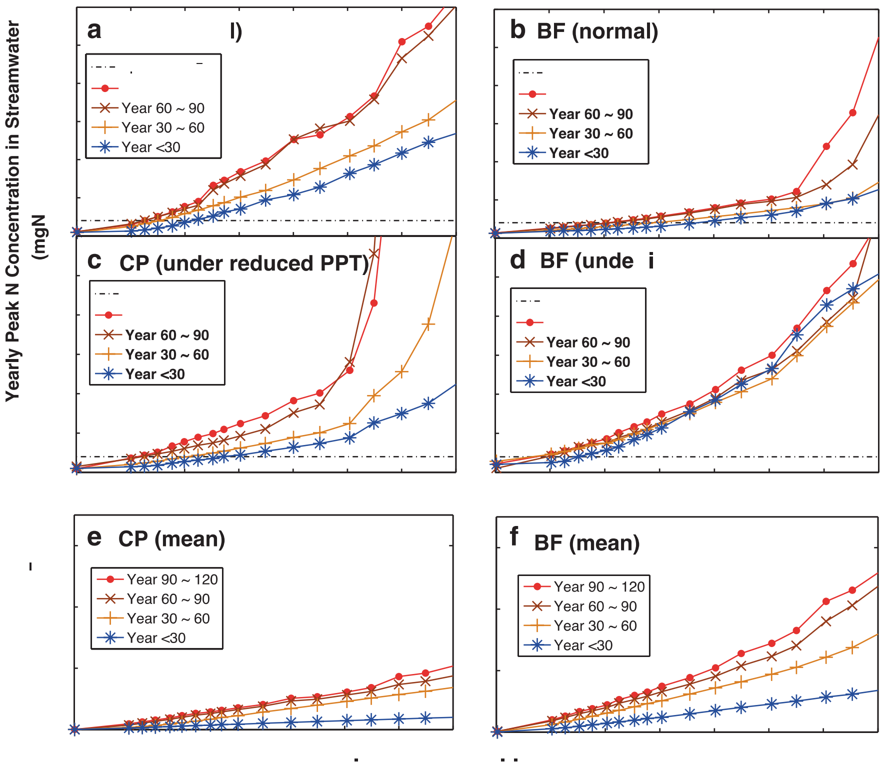

Fig. 10.1 DayCent simulated trends in annual peak NO_3–N concentrations in streamwater and annual mean gaseous emissions of N from soil that occurred within various time periods since elevated N deposition began in 1940. In these simulations N deposition since 1940 ranged from 0 to 80 kg N $ha^{-1}yr^{-1}$. The model was parameterized for the Camp Paivika (CP; plots **a**, **c** and **e**) and Barton Flats (BF; plots **b**, **d** and **f**) sites in the San Bernardino National Forest in southern California, USA. The effect of normal or altered precipitation levels on simulated nitrate leaching is shown in plots **a**–**d**. The prescribed N deposition values were set with < 10 % random variation. (Modified from Fenn et al. 2008)

17–20 % of the atmospherically deposited N was re-emitted as NO and N_2O (Gasche and Papen 2002; Skiba et al. 2004).

10.3 Desert Scrub and Pinyon-Juniper Woodland

Desert ecosystems downwind of urban and agricultural centers can receive N deposition as high as 30 kg $ha^{-1}yr^{-1}$ (Fenn et al. 2003). For these ecosystems, CLs cannot be set using the traditional endpoints of NO_3^- leaching or soil acidification due to the high alkalinity of the soils and the propensity of the nitrogen to be leached deep into the soil profile where it is sequestered (Walvoord et al. 2003). Instead, deposited N has a fertilization effect that promotes the production of the fast-growing ephemeral herbaceous community.

Increased production of these annual forbs and grasses has been correlated with increased frequency and intensity of fires (Brown and Minnich 1986), due in large part to the invasion of exotic annual grasses. These exotic grasses create a continuous fine fuel load that allows fires to spread rapidly through the landscape, resulting in severe damage to the ecosystem (Brooks et al. 2004). Although the amount of fine fuel necessary to carry fire in the desert is currently unknown, studies evaluating this threshold are underway, and in grassland ecosystems 1000 kg ha^{-1} of fine fuel dry mass can carry fire (Anderson 1982). Exotic grasses may also outcompete native annuals due to the plastic response of these exotics to increased resource availability (DeFalco et al. 2003; Steers and Allen 2010). Thus, CLs for southern California desert communities can be set using both the amount of N needed to increase exotic grasses and decrease native annuals, and the amount of N needed to increase herbaceous biomass production above the fire-carrying threshold. Here we provide results for both types of CL using empirical and modelling methodologies.

10.3.1 Methodologies for Empirical and Model-based CLs in View of Fire Risk

For the empirical study, four sites were selected in Joshua Tree National Park (JTNP) that span a N deposition gradient. Two sites were located in creosote bush scrub (CBS) and two sites were in pinyon-juniper woodland (PJW). Nitrogen fertilizer was applied each winter at rates of 0, 5, and 30 kg ha^{-1} for five consecutive years beginning in 2002. Nitrogen deposition along the gradient ranged from 3.4 to 12.4 kg N ha^{-1}yr^{-1} as measured by ion exchange resin bulk throughfall deposition samplers (Fenn et al. 2009) and confirmed with CMAQ model simulations (Tonnesen et al. 2007). The empirical CL was determined as the lowest N treatment plus background N deposition that increased total winter biomass above the fire threshold and/or caused increased invasive grass biomass and decreased native richness. Plots were sampled for richness and percent cover of native and exotic annuals at the time of peak production. Biomass was estimated using biomass-to-percent cover regressions (see Allen et al. 2009; Rao and Allen 2010 for detailed methods).

CLs were also determined for CBS and PJW by DayCent model simulations of winter annual vegetation production under a range of soil textures, precipitation regimes, and N deposition levels (Rao et al. 2010). The model was calibrated and validated using soil profile, plant chemistry, and biomass data from the four fertilization sites in JTNP. Once parameterized for each vegetation type, winter annual biomass production under increasing N-deposition loads was modelled. Production was simulated for 100 years at each N deposition load, and the fire risk at each load was determined as the fraction of years in which the fire threshold was exceeded. The CL was defined as the N-deposition load at which the fire risk began increasing exponentially above the background fire risk (Fig. 10.2). The amount of N deposition at which fire risk no longer increased with added N was termed the fire risk

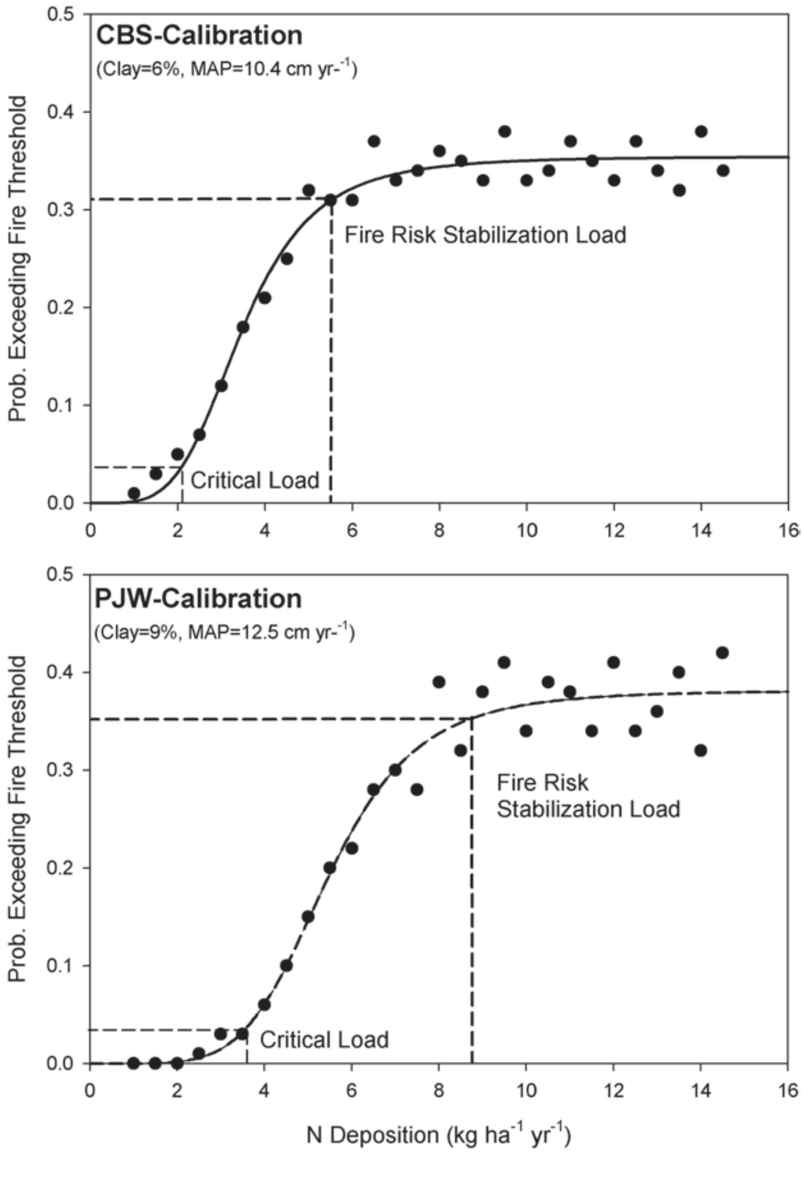

Fig. 10.2 Examples of fire risk for the model calibration sites from each vegetation type, which was calculated as the probability that annual biomass will exceed the fire threshold under a given N deposition load. For these sites, the CLs are 2.1 and 3.6 kg ha^{-1}yr^{-1} of N deposition for creosote bush scrub (CBS) and pinyon-juniper woodland (PJW) respectively. The fire risk begins to level out at the stabilization load (SL), which is 5.5 and 8.8 kg ha^{-1}yr^{-1} of N deposition for CBS and PJW, respectively. Between the CL and SL the fire risk changes very rapidly with increases or decreases in N deposition. *MAP* mean annual precipitation

stabilization load (SL). Above the SL, fire risk is controlled by variation in annual precipitation and does not increase with increased N deposition, although annual biomass production will still increase with added N (Rao and Allen 2010). The CLs and SLs were calculated for six precipitation regimes and six soil textures that bracketed observations from the region.

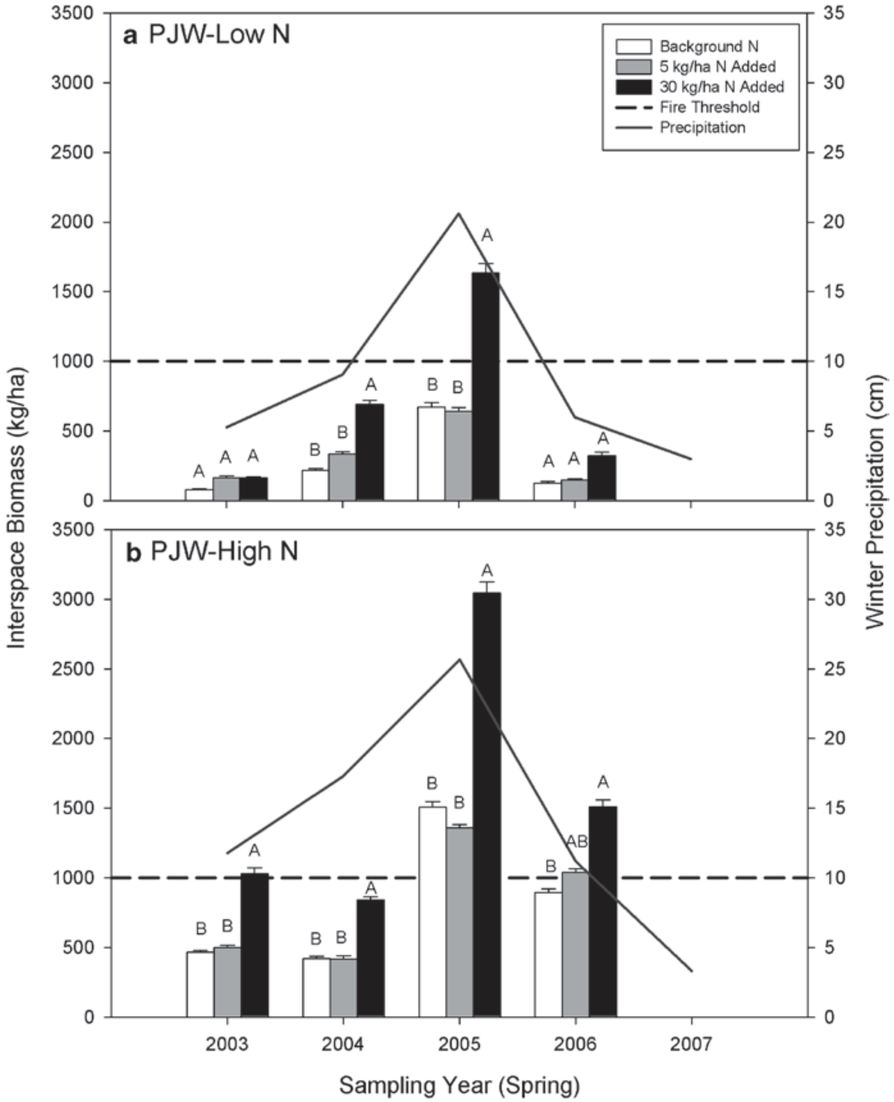

Fig. 10.3 Changes in total interspace (herbaceous) biomass with N fertilization and yearly differences in precipitation at four sites (*A* pinyon-juniper woodland (PJW) low N-deposition; *B* PJW high N-deposition; *C* creosote bush scrub (CBS) low N-deposition; *D* CBS high N-deposition). Letters above bars indicate Significant differences in soil concentrations within years. In all cases significance was determined using the post hoc test Tukey's HSD at α 0.05

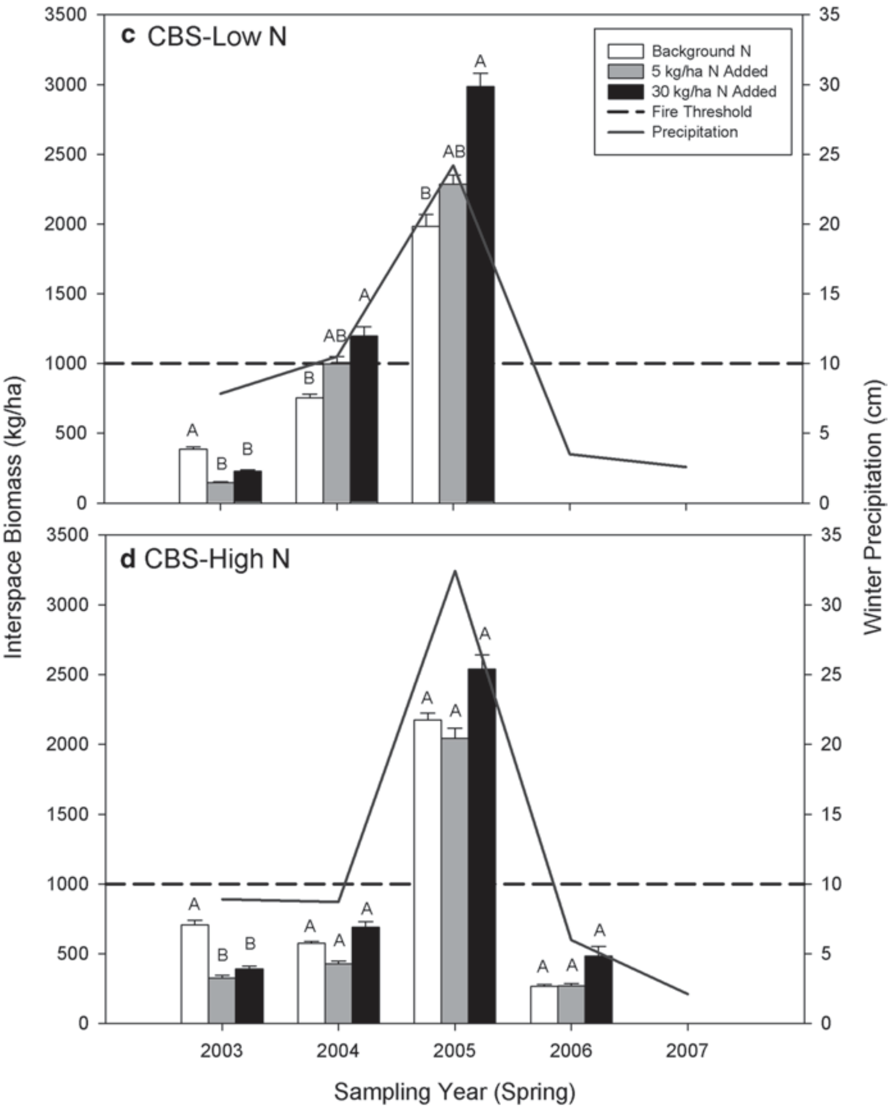

Fig. 10.3 (Continued)

10.3.2 Empirical and Model-based CLs for Desert Scrub and Pinyon-Juniper Woodland

The empirical CL calculations were somewhat confounded by the fact that both production and relative abundance of exotic and native annuals were influenced by the interaction between N fertilization and precipitation. For the CL based on fine fuel production, high precipitation resulted in biomass production above the fire threshold regardless of N fertilization level (Fig. 10.3b–d). However, in four instances under average precipitation the addition of N at 5 or 30 kg N ha^{-1} pushed the biomass above the fire threshold (Fig. 10.3a–c). Invasive grasses increased and native forbs generally decreased under both 5 and 30 kg N ha^{-1} fertilizer additions at two of the four sites in the wet year of 2005. In a drier year only 30 kg N ha^{-1} caused an increase in invasive grasses in two of the four sites. Using the background deposition value for the site with the least amount of N deposition that demonstrated an effect of fertilization, we can calculate the CL for the impact of invasive grasses on native forbs as 8 kg N ha^{-1} (5 kg N ha^{-1} added + 3 kg N ha^{-1} background deposition). The empirical CL based on fine fuel accumulation is likely at the same level, but could not be determined due to precipitation-limited production during most years of our study.

The DayCent model results indicate that above the CLs of these ecosystems, small increases in N deposition result in large increases in fire risk up to the SL. For CBS, the average SL over six soil textures and four precipitation regimes was 8.15 kg $ha^{-1}yr^{-1}$. This value is very similar to the CL for increased exotic species and decreased native species cover determined empirically through the fertilization experiment, suggesting that this level of N deposition will be detrimental to both diversity and fire dynamics. As with the empirical CLs, the modelled CLs were highly variable across different precipitation regimes (Rao et al. 2010).

The CL and SL for PJW were lower than those for CBS because PJW is more likely to burn than CBS due to the greater abundance of woody biomass (Brooks and Minnich 2006). The low N deposition levels that result in increased fire risk at PJW suggests that much of this ecosystem type in California is at high risk of fire due to the combination of increased fine fuel production caused by atmospheric N deposition and inherently high woody fuel abundance. In summary, the empirical CL for exotic grass invasion in desert ecosystems is 8 kg $ha^{-1}yr^{-1}$. Based on the DayCent simulations, the range including the lower and upper bounds of the CLs for CBS and PJW are 3.2–9.3 and 3.0–6.3 kg $ha^{-1}yr^{-1}$ respectively, depending on soil texture and precipitation regime (Rao et al. 2010).

10.4 High Elevation Catchments of the Colorado Rocky Mountains

The Front Range of the Rocky Mountains includes the high peaks of the American Cordillera that rise from the Great Plains of Colorado to elevations in excess of 3000 m in very short lateral distances (less than 30 km). Mountain areas above tree line are especially susceptible to changes in atmospheric inputs of N and other atmospheric contaminants. This susceptibility is predicated on the low biomass, and thin soils of these ecosystems. Episodic acidification and surface water ANC values below zero have been reported in high elevation catchments in the Front Range, likely due to the dilute nature of waters at the highest elevations, shallow soils and short residence times of drainage water in these ecosystems. Nutrient N effects on these systems have also been documented, and both mechanistic and empirical modelling approaches have been used to establish CLs in these high elevation catchments.

10.4.1 Methodologies for Empirical and Model-based CLs for Nitrate Leaching, Acidification and Biodiversity Impacts

Williams and Tonnessen (2000) estimated the empirical acidification CL for lakes of the Colorado Front Range based on NADP wet deposition monitoring and the combined results of the U.S. Environmental Protection Agency Western Lakes Survey and a more focused survey of 91 lakes in the Front Range. Their approach was to examine the pH, ANC, and NO_3^- concentration distributions within the two populations of lakes in connection with wet deposition data across the intermountain western states.

Baron et al. (2011a) used lake surveys and deposition data to estimate empirical CLs of N by plotting lake NO_3^- concentrations (n 285 for the Rocky Mountains) vs. N deposition and inferring the inflection point or threshold at which NO_3^- concentrations increased in response to N deposition. Using a different approach, Baron (2006) estimated an empirical CL from historical reconstructions of atmospheric wet deposition to 1900. She combined these hindcasts with data on the diatom communities of lakes in Rocky Mountain National Park (RMNP) to set the CL at the estimated deposition rate during the period 1950–1964 when alteration of diatom assemblages was inferred from analysis of sediment cores collected from alpine lakes in RMNP (Wolfe et al. 2003).

Using the MAGIC model Sullivan et al. (2005) estimated the N and S CLs for surface water acidification in the Colorado Front Range. The MAGIC model assumes that a catchment can be modelled as a lumped reactive soil that contains N biogeochemistry and soil geochemical exchange and weathering reactions. The CLs were estimated by simulating deposition impacts on surface water ANC and pH. Hartmann et al. (2007, 2009) simulated biology, hydrology and geochemistry for two catchments in the Front Range with the DayCent-Chem model. The study highlighted the need to capture both the biological and geochemical system response in order to properly estimate the sensitivity of alpine ecosystems to atmospheric deposition. While the study itself does not explicitly address CLs, the results include modelled estimates and current conditions of acidification and NO_3^- concentrations in both the Andrews Creek (RMNP) and Green Lakes Valley (Niwot Ridge) watersheds (Hartman et al. 2009). Based on atmospheric deposition levels at the two sites (Hartman et al. 2009), an approximation of the N CL can be determined.

Empirical and modelled CLs were also determined for plant species change and biodiversity impacts to alpine vegetation in the Rocky Mountains (Bowman et al. 2006; Sverdrup et al. 2012). The empirical CL was determined from N fertilization experiments (0, 20, 40 and 60 kg N $ha^{-1}yr^{-1}$) in an alpine dry meadow at Niwot Ridge over an 8-year period (Bowman et al. 2006). The simulated CL for biodiversity effects was produced using the ForSAFE-VEG model parameterized for a generalized site in the alpine and subalpine zones of the northern and central Rocky Mountains for the years 1750–2500 (Sverdrup et al. 2012). The ForSAFE-VEG model includes modules to simulate soil chemistry, hydrology, energy, C and N cycling, tree growth and production, geochemistry and ground vegetation (Sverdrup et al. 2012). The VEG submodel includes dynamic competition principles for interspecies interactions.

10.4.2 Empirical and Model-based CLs for the Colorado Rocky Mountains

The empirical CL for NO_3^- leaching based on a survey of lakes in the Rocky Mountains was 3.0 kg N $ha^{-1}yr^{-1}$ (Baron et al. 2011a). Baron et al. (1994) simulated stream N export with increasing N deposition in the Loch Vale Watershed in RMNP with the Century model and reported a threshold for increased N export at a N deposition of 2–3 kg N $ha^{-1}yr^{-1}$. This CL is in close agreement with the empirical CL (Baron et al. 2011a; Table 10.1). Paleolimnological hindcast studies in high elevation lakes of the Colorado Front Range (Baron 2006; Wolfe et al. 2003), the eastern Sierra Nevada of California and the Central Rocky Mountains indicate an empirical N CL of 1.4–1.5 kg N $ha^{-1}yr^{-1}$ for effects on phytoplankton communities (Saros et al. 2011).

Field surveys and N enrichment studies have shown that alpine lake NO_3^- concentrations within the range of 3–12 µmol l^{-1} are associated with increased phytoplankton biomass, changes in phytoplankton communities, and a shift to P limitation (Bergström and Jannson 2006; Elser et al. 2009; Interlandi and Kilham 2001). DayCent-Chem simulations of streamwater NO_3^- concentrations for Andrews Creek and Niwot Ridge indicated streamwater NO_3^- concentrations typically ranging from 0 to 100 µmol l^{-1}, similar to empirical data (2–60 µmol l^{-1}) for the same sites (Hartman et al. 2009). With field and simulated NO_3^- values indicative of elevated NO_3^- leaching and with NO_3^- concentrations much higher than those known to affect phytoplankton communities, we conclude that these sites (N deposition levels of 3.6 and 5.9 kg $ha^{-1}yr^{-1}$) are in exceedance of the N CL. Further DayCent-Chem simulations with atmospheric N inputs varying over the appropriate range are needed to refine the simulated N deposition CL for nutrient enrichment.

The empirical CL estimates for lake acidification of 4 kg N $ha^{-1}yr^{-1}$ as wet deposition (Williams and Tonnessen 2000) and 4 kg N $ha^{-1}yr^{-1}$ as total inorganic N deposition (Baron et al. 2011a) are within the margin of error, particularly for estimating N deposition in this region where dry deposition is purported to constitute only 15 % of the total (Baron et al. 2011a). The MAGIC model yielded an acidification CL of 7.8 kg N $ha^{-1}yr^{-1}$ at Andrews Creek based on an ANC of 20 µeq l^{-1}, and a CL of 12 kg N $ha^{-1}yr^{-1}$ for the Loch, which is not among the most acid-sensitive lakes in the region (Sullivan et al. 2005). These simulated acidification CLs are higher than the empirical acidification CL, but not all lakes are equally sensitive (Sullivan et al. 2005). If a threshold ANC of 20 µeq l^{-1} is chosen for estimating the CL, the

Table 10.1 A comparison of empirical and simulated critical loads for alpine ecosystems in the Rocky Mountains, Colorado, USA

Acidification or N enrichment CL	Empirical or modelled CL	Response indicator	CL value (kg N $ha^{-1}yr^{-1}$)	References
Catchment-level responses				
Acidification	Empirical	ANC	4	(Baron et al. 2011a; Williams and Tonnessen 2000)
	Modelled (MAGIC model)	ANC	7.8–12.0	(Sullivan et al. 2005)
N enrichment	Empirical	Change in diatom assemblages	1.4–1.5	(Baron 2006; Saros et al. 2011; Wolfe et al. 2003)
	Empirical	Surface water NO_3 concentrations	3	(Baron et al. 2011a)
	Modelled (century)	Stream N export	2–3	(Baron et al. 1994)
	Modelled (DayCent-Chem model)[a]	Surface water NO_3 concentrations	≤3.6–5.9	(Hartman et al. 2007, 2009)
Terrestrial vegetation responses				
N enrichment	Empirical	Change in individual plant species	4	(Bowman et al. 2006)
	Empirical	Plant community change	10	(Bowman et al. 2006)
	Modelled (ForSAFE-VEG model)	Long-term plant biodiversity change	1–2	(Sverdrup et al. 2012)

[a] DayCent-Chem simulations of Hartman et al. (2007, 2009) were not explicitly designed to determine a CL. Thus, the CL estimates are based on the known atmospheric deposition (kg ha^{-1} yr^{-1}) at the sites for which the model runs were parameterized.

empirical CL for acidification is not exceeded at Andrews Creek where N deposition is 3.6 kg $ha^{-1}yr^{-1}$, nor at Niwot Ridge where N deposition is 5.9 kg $ha^{-1}yr^{-1}$. These empirical data suggest that at some sites the acidification CL is higher than the proposed empirical CL value of 4 kg N $ha^{-1}yr^{-1}$.

Modelling stream ANC for determining acidification CLs with the DayCent-Chem model would benefit from model refinement. Modelling stream ANC and pH was challenging because these parameters were highly sensitive to complex silica reactions and stream pCO_2 (Hartman et al. 2007). Simulated daily ANC concentrations were also sensitive to daily discharge estimates and when discharge was overestimated ANC was underestimated and vice versa. Simulations of ANC with DayCent-Chem did not always track well with empirical data, although simulated annual volume-weighted mean ANC concentration was within 12 μeq l^{-1} of the measured mean (Hartman et al. 2009).

The empirical CL for changes to individual alpine plant species was 4 kg N $ha^{-1}yr^{-1}$, compared to 10 kg N $ha^{-1}yr^{-1}$ for overall plant community change based on an 8 year fertilization study at Niwot Ridge (Bowman et al. 2006). In comparison, the ForSAFE-VEG model estimated a biodiversity CL of 1–2 kg N $ha^{-1}yr^{-1}$ for a generalized Rocky Mountain alpine site (Sverdrup et al. 2012). The simulated N CL could be higher if different parameterization values are used for precipitation, temperature, soil chemistry, plant nutrient uptake or by altering the amount of biodiversity change considered acceptable. The lower CL derived from the ForSAFE-VEG model is presumably largely due to the much longer time scale for the impacts of N to take effect compared to the fertilization study. An additional factor is that the CL for N deposition effects on alpine plant communities is already exceeded at the study site based on the estimated ambient N deposition (6 kg $ha^{-1}yr^{-1}$; Bowman et al. 2006).

In these studies in the Colorado Rocky Mountains, both empirical and simulated CL values were higher for acidification effects than for nutrient-N effects, as is commonly reported (Hettelingh et al. 2008). The empirical N CL for surface water acidification (4 kg N $ha^{-1}yr^{-1}$) is higher than the empirical CL for nutrient effects (2–3 kg N $ha^{-1}yr^{-1}$ for elevated NO_3^-; 1.5 kg N $ha^{-1}yr^{-1}$ for effects on diatom assemblages; Table 10.1). Likewise, the simulated CL for acidification using the MAGIC model (7.8 at Andrews Creek and 12.0 at the Loch) is higher than the simulated CL for nutrient N based on DayCent-Chem (<3.6 kg N $ha^{-1}yr^{-1}$; Table 10.1). However, in the latter case, N deposition inputs were not varied to explicitly determine the CL. Note that only in the case of the empirical N enrichment CL (Baron 2006) was a biological indicator used (alteration of algal assemblages) to estimate the CL for surface waters or catchment-level responses (Table 10.1). Both empirical and modelling approaches for determining CLs are useful, and are complimentary and reinforcing each other.

10.5 Adirondack Lake Watersheds in New York State

The Adirondack Mountain region is arguably among the regions of the U.S. most highly impacted by acidic deposition (Driscoll et al. 1991). The Adirondack Park encompasses 2.4 million ha in northern New York, with about 1 million ha of publicly owned state lands and 1.4 million ha of private lands. The region is a unique landscape of forested uplands and wetlands, and includes approximately 2800 lakes (>0.2 ha). The Adirondacks receive elevated inputs of atmospheric S, NO_3^- and ammonium (NH_4^+) deposition (Driscoll et al. 1991). In 1984–1987 the Adirondack Lakes Survey determined that 26 % of 1469 surveyed lakes had pH <5.0, 26 % had ANC <0 μeq l^{-1}, and 50 % had ANC <50 μeq l^{-1} (Kretser et al. 1989). As a result, there are 128 lakes in the Adirondacks that are included on the New York State Section List because of impairment to aquatic life attributed to acidic deposition (based on the criterion of pH <6.0; www.dec.ny.gov/chemical/31290.html). The acidic conditions in acid-sensitive Adirondack lakes are due to elevated leaching of sulfate (SO_4^{2-}) and NO_3^- in surface waters relative to the supply of base cations from the watershed (Driscoll et al. 1991). There is considerable interest in the application of models and the development of empirical relationships to determine CLs or total maximum daily loads (TMDLs) with respect to lake acidity in this region.

The objective of this case study was to illustrate the use of a dynamic model (PnET-BGC) in the calculation of CLs for lake watersheds in the Adirondack region of New York. We examine the tradeoffs of controls of (SO_4^{2-}) deposition versus NO_3^- deposition. Note that PnET-BGC is capable of simulating the effects of changes in NH_4^+ deposition, but for this chapter we chose to evaluate changes in (SO_4^{2-}) and NO_3^- deposition, the focus of current emissions control programs for acidic deposition in the U.S. (USEPA 2009). We have observed only minor differences in the response of Adirondack soils and surface waters between equivalent changes in NO_3^- and NH_4^+ deposition in simulations with PnET-BGC. We also compare and relate the use of dynamic models with empirical approaches to calculate CLs.

10.5.1 Methodologies for Model-based CLs for Nitrate Leaching and Acidification

PnET-BGC was applied to 20 lakes of the Adirondack Long-Term Monitoring (ALTM) Program (Driscoll et al. 2003) to evaluate CLs of acidity and N for the region. These lakes and their watersheds exhibit a range of characteristics and sensitivity to acidic deposition. For the 20 ALTM lake-watersheds, we show model simulations that compare results of the dynamic model PnET-BGC with empirical approaches that have been used to assess CLs of surface waters. To illustrate the use of model calculations for the determination of CLs, we show results from Jockeybush Lake (43°18'N, 74°35'W), a thin till drainage lake with a forested catchment. Jockeybush Lake has been monitored for lake chemistry since 1992 (Driscoll et al. 2003). It is chronically acidic and has a mean $SO_4^{2-} = 92\,\mu eq\,l^{-1}$, NO_3^- 17 µeq l^{-1}, ANC 4.5 µeq l^{-1} and pH 5.4.

Model Description PnET-BGC is a comprehensive forest-soil-water model that links a C, N and water balance model, PnET-CN (Aber et al. 1997), with a biogeochemical model, BGC (Gbondo-Tugbawa et al. 2001). The model performs well in small, high-elevation watersheds where detailed site data are available to constrain inputs and parameter values, but regional scale applications have also been conducted (Chen and Driscoll 2004, 2005; Zhai et al. 2008).

PnET-BGC extends the simulations of PnET-CN to include the cycling of all major elements (i.e., C, N, P, S, Ca, Mg, K, Na, Al, Cl, Si). Both major biotic and abiotic processes are represented in PnET-BGC, including atmospheric deposition, canopy interaction, CO_2 fertilization, litterfall, forest growth, root uptake, snowpack accumulation and loss, routing of water along hydrologic flowpaths, soil organic matter dynamics, nitrogen mineralization and nitrification, mineral weathering, wetland biogeochemical processes, chemical reactions involving solid and solution phases, and surface water processes. The model can be run on a time step specified by the user; a monthly time step was used for this study.

PnET-BGC requires input parameters related to the site: meteorological conditions, atmospheric deposition, element weathering, soils and vegetation and land-disturbance history. Basic soil parameters needed for PnET-BGC include properties such as soil mass, cation exchange capacity, cation exchange constants and anion adsorption constants. Vegetation is characterized in PnET-BGC using the major forest cover types represented at the study site and the element stoichiometry associated with these cover types (Gbondo-Tugbawa et al. 2001).

Model Calibration and Application Following previous research (Zhai et al. 2008), model runs for Jockeybush Lake were started in the year 1000 AD, and run under constant pre-industrial deposition and no land disturbance until 1850 to achieve steady-state and evaluate "background" (i.e., pre -1850) conditions. Changes in atmospheric deposition and land disturbance events were initiated after 1850. The model was run from 1850 through 2010 based on measured values of atmospheric deposition and reconstructions of historical deposition from emission records (Fig. 10.4a, b; Driscoll et al. 2001, Zhai et al. 2008). For the period 1978–2010, we estimated atmospheric deposition from measured wet deposition values at Huntington Forest (44°00'W, 74°13'N; NADP NY20) in the central Adirondacks. For the period before 1850, we assumed that atmospheric deposition was 10% of current values. For the period 1978–1900, we used empirical relations between atmospheric anthropogenic emissions for the atmospheric source area of the Adirondacks and the measured atmospheric deposition data for Huntington Forest (1978–2010) to reconstruct deposition based on historical emission records for the period. For the period between 1850 and 1900, we assumed a linear increase in atmospheric deposition from background values. To estimate total deposition from wet deposition we assume a fixed dry to wet deposition ratio based on dry deposition measurements at Huntington Forest. To extrapolate these estimates of atmospheric historical deposition for Huntington Forest to Jockeybush Lake watershed, we used the spatial deposition model of Ito et al. (2002). Model simulations continued to the year 2200 with a series of forecasts which included a range of deposition scenarios from current to "background" deposition for SO_4^{2-}, and NO_3^- individually and in combination. This range corresponds to 0–100% decreases in anthropogenic atmospheric SO_4^{2-} and NO_3^- deposition. Future scenarios involved a 10 year ramp from current values to the level of deposition of interest and continued simulation at this deposition level to 2200 (Fig. 10.4a, b). This range of values enabled evaluation of tradeoffs associated with reductions in sulfur dioxide, and nitrogen oxides to achieve ecosystem recovery from acidic deposition.

10.5.2 Empirical and Model-based CLs for Adirondack Lake Watersheds

The model hindcast for Jockeybush Lake suggests that prior to the advent of acidic deposition, the ANC was approximately 60 μeq l^{-1} (Fig. 10.4c–e). With increases

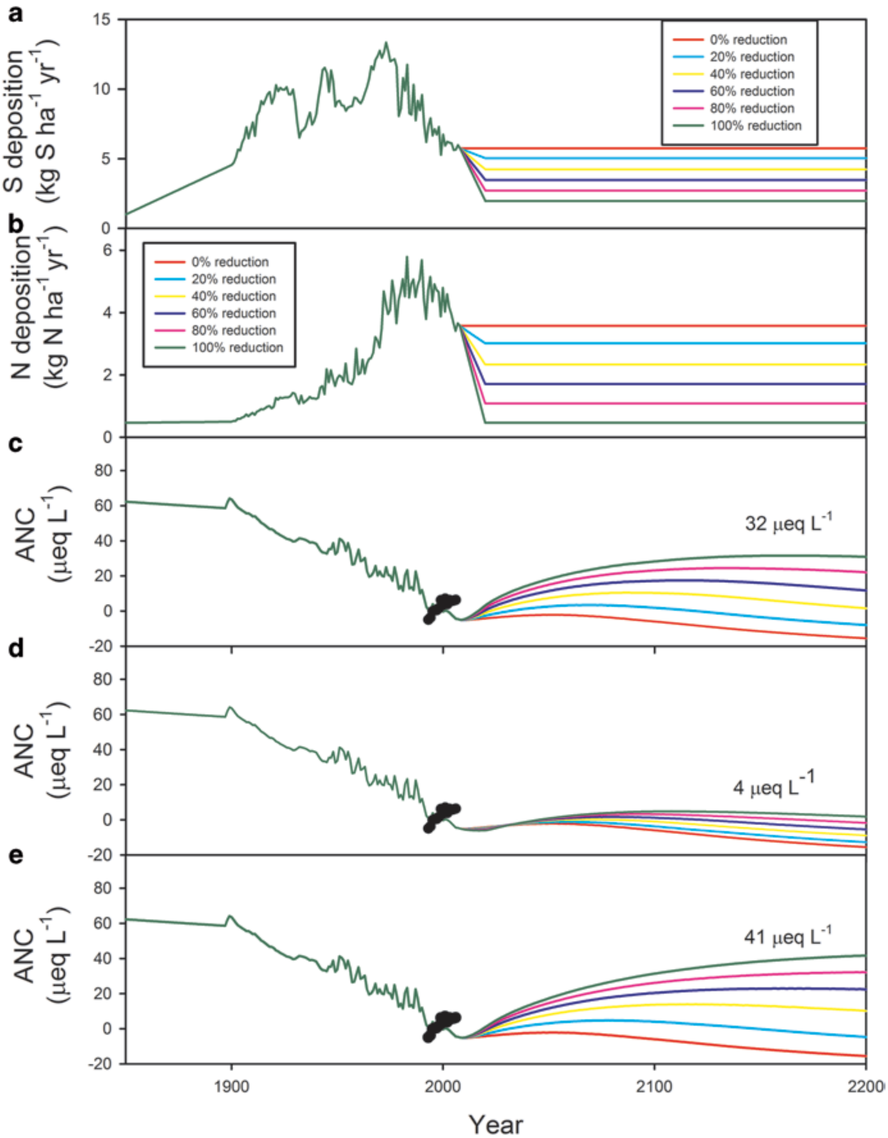

Fig. 10.4 Time-series of model inputs of atmospheric sulfur (S) (**a**) and nitrate (NO_3^-) (**b**) deposition for Jockeybush Lake and model simulations of lake acid neutralizing capacity (ANC) hindcast (1950–2010) and model projections (2010–2200) under a suite of decreases in S (**c**), NO_3^- (**d**), and S + NO_3^- (**e**) deposition, corresponding to 0–100 % decreases in anthropogenic S and NO_3^- deposition. Measured values of ANC are shown as *black dots*

in atmospheric SO_4^{2-} and NO_3^- deposition through the twentieth Century, model simulation indicate that ANC decreased to approximately zero (−4 μeq l^{-1}). The simulated loss of ANC for the lake is similar to regional values reported previously (Zhai et al. 2008).

Model forecasts for Jockeybush Lake were conducted for a series of future scenarios of SO_4^{2-} and NO_3^- deposition ranging from no reduction from current deposition (no reduction) to complete elimination of anthropogenic deposition and decreases to "background" (pre-anthropogenic) deposition (100 % reduction; Fig. 10.4a, b). A range of recoveries of ANC are projected coinciding with the range of deposition scenarios (Fig. 10.4c–e). Projections of lake ANC responses are initially relatively rapid following decreases in SO_4^{2-} loading but not to decreases in NO_3^- loading. The rate of ANC increase subsequently decreases as the watershed approaches steady-state with respect to the lower input of atmospheric SO_4^{2-} or NO_3^- deposition. Note under the lower projections of decreases in atmospheric deposition (e.g., 0, 20 %) following an initial period of partial recovery, the lake ANC ultimately decreases. The reason for this projected re-acidification is two-fold. First, limited decreases in atmospheric deposition are not large enough to reverse the net loss of exchangeable calcium and magnesium from the soil, and the continued acidification of soil ultimately contributes to the acidification of the drainage water. Second, the PnET-BGC simulates an aggrading forest. As the forest ages, its demand for N decreases and NO_3^- leaching increases. This stand age-dependent retention of N and leaching of NO_3^- also contributes to the re-acidification of lake water.

Model projections suggest that under no additional controls of SO_4^{2-} or NO_3^- deposition (0 % reduction) the ANC of Jockeybush Lake will continue to acidify to −15 μeq l^{-1} by 2200 (Fig. 10.4e). In contrast, if anthropogenic atmospheric SO_4^{2-} deposition is eliminated (100 % reduction) with no change in atmospheric NO_3^- deposition, the ANC is projected to increase to 32 μeq l^{-1} by 2200 (Fig. 10.4c). Note that even under the scenario of complete elimination of atmospheric SO_4^{2-} deposition, Jockeybush Lake does not recover its pre-anthropogenic ANC (~60 μeq l^{-1}) by 2200. This net loss of ANC is due to soil acidification associated with the net depletion of exchangeable calcium and magnesium in soil from historical acidic deposition.

The projected lake responses to decreases in atmospheric NO_3^- deposition were similar to SO_4^{2-} responses, but considerably more muted. If anthropogenic atmospheric NO_3^- deposition is eliminated (100 % reduction) with no change in atmospheric SO_4^{2-} deposition, the ANC is projected to increase only to 4 μeq l^{-1} by 2200. This analysis indicates that controls on atmospheric SO_4^{2-} deposition are more effective in facilitating increases in ANC than decreases in NO_3^- deposition in Adirondack watersheds.

The projections of lake responses to decreases in future SO_4^{2-} and NO_3^- in combination show greater increases in ANC than decreases in SO_4^{2-} alone (up to 41 μeq l^{-1} for 100 % reduction; Fig. 10.4e). These simulations suggest that there are benefits associated with simultaneous controls of SO_4^{2-} and NO_3^- in achieving increases in ANC.

Comparison of Model Results with Approaches for Empirical Critical Loads In this analysis, we consider two approaches for evaluating empirical vs. modelled CLs for NO_3^- leaching and acidification by using simulation data for the 20 ALTM lakes. The empirical CL for NO_3^- leaching is based on field observations of surface water NO_3^- concentrations which typically exhibit a "dogleg" pattern in response to increases in atmospheric N deposition (Aber et al. 2003). The "dogleg" pattern is manifested by low surface water concentrations of NO_3^- at lower levels of atmospheric N deposition and at a critical load some waters show a pattern of increases in NO_3^- with increases in deposition. This leaching response is highly variable in watersheds receiving elevated N deposition due to historical land disturbance, and vegetation and land cover characteristics (Aber et al. 2003; Baron et al. 2011b). These empirical observations are typically obtained from surface water data for many sites along a spatial gradient of atmospheric N deposition. This "dogleg" pattern of watershed response to variations in N deposition has been reported for Europe and the eastern and western U.S. (Baron et al. 2011b) and has been used in the determination of empirical CLs for surface waters (Pardo et al. 2011). For example, Aber et al. (2003) observed this pattern of NO_3^- response to variation in atmospheric N deposition for surface waters in the northeastern U.S, including the Adirondacks, and found that the critical load of N above which elevated leaching of NO_3^- could occur was 8 kg N $ha^{-1}yr^{-1}$. Aber et al. (2003) observed maximum surface water NO_3^- concentrations of 30–40 µmol l^{-1} at the highest observations of N deposition of 10–12 kg N $ha^{-1}yr^{-1}$. The assumption that is inherent in the use of these empirical relations for CLs is that the observed spatial pattern of NO_3^- leaching is indicative of the temporal response that would occur in response to changes in N deposition at a given site (i.e. space-for-time substitution; e.g., Aber et al. 2003).

We used results of PnET-BGC simulations for the 20 ALTM watersheds to evaluate whether the pattern of NO_3^- leaching with changes in N deposition was similar to empirical observations, such as those reported by Aber et al. (2003). We averaged time-series of lake NO_3^- simulations over 10-year intervals for each of the ALTM lakes over the period of hindcasts (1850–2010; 16 observations per site). Thus, the results of PnET-BGC runs capture both spatial (20 sites) and temporal (time series hindcast) simulated NO_3^- response to changes in N deposition.

In contrast to the "dogleg" pattern typical of empirical observations, PnET-BGC simulations generally showed a linear pattern of increase in NO_3^- concentrations in response to increases in N deposition to Adirondack lake-watersheds (Fig. 10.5; according to the equation, NO_3^- (µmol l^{-1}) 2.9 × total N deposition (kg N $ha^{-1}yr^{-1}$)+2.7; r^2 0.55). As for the empirical data (Aber et al. 2003; Baron et al. 2011a) there was considerable variability around this "linear" relationship. Some of the simulation periods for some of the ALTM sites corresponded with the time period shortly after a land disturbance event (e.g., cutting, blowdown; noted in Fig. 10.5 as land disturbance). PnET-BGC simulates elevated NO_3^- leaching associated with land disturbance events and these observations are depicted as outliers in Fig. 10.5. Given this approximately linear pattern of NO_3^- leaching in response to changes in N deposition from PnET-BGC simulations, a CL for N could be estimated by specifying an acceptable level of leaching. For example, Gundersen et al.

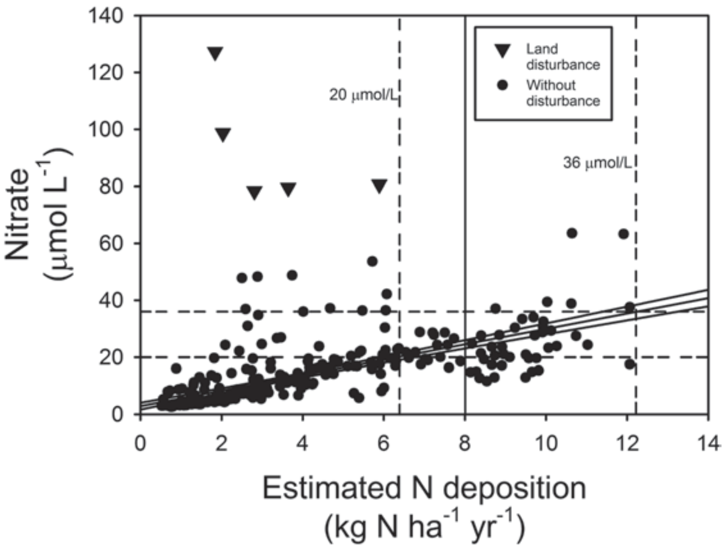

Fig. 10.5 Simulated response of 10 year average concentrations of nitrate to changes in atmospheric NO_3^- deposition over the 1850–2010 hindcast period for 20 Adirondack lake watersheds. Outlier observations are shown which represent simulated conditions shortly after land disturbance events (e.g., clear-cutting, blowdowns). A linear regression of simulated nitrate as a function of N deposition is shown with 95% confidence interval is shown (NO_3^- (µmol l^{-1}) 2.9 × total N deposition (kg N $ha^{-1}yr^{-1}$)+2.7; r^2 0.55). Using this regression, CLs are estimated for lake nitrate of 20 and 36 µmol l^{-1} (shown with *dashed vertical lines*) at 6.4 kg N $ha^{-1}yr^{-1}$ and 12.2 kg N $ha^{-1}yr^{-1}$, respectively. A *vertical line* is also shown at 8 kg N $ha^{-1}yr^{-1}$ to indicate the level of atmospheric deposition where elevated nitrate leaching approximately occurs from empirical spatial observations

(2006) proposed a threshold for annual mean surface water NO_3^- of 36 µmol l^{-1} that is thought to be indicative of a "leaky" watershed (based on data from North America and Europe). More recently, Fenn et al. (2011) suggested a threshold of 20 µmol l^{-1} for US watershed in the determination of empirical CLs. Invoking these NO_3^- concentration limits to the PnET-BGC-derived relationship for NO_3^- leaching response to varying atmospheric N deposition of Adirondack lake-watersheds, a CL of 6.4 kg N $ha^{-1}yr^{-1}$ and 12.2 kg N $ha^{-1}yr^{-1}$ were obtained for NO_3^- thresholds of 20 µmol l^{-1} and 36 µmol l^{-1}, respectively (Fig. 10.5) in general agreement with the value of 8 kg N $ha^{-1}yr^{-1}$ suggested for northeastern U.S. surface waters (Pardo et al. 2011).

Empirical approaches have also been used to evaluate CLs of acidity for surface waters. The empirical F-factor has been used in steady-state CL applications (e.g., USEPA 2009). The F-factor is the ratio of the change over time in the sum of concentration of base cations (C_B) divided by the change in $SO_4^{2-} + NO_3^-$ concentration (C_A) relative to the pre-industrial steady-state water chemistry condition.

Invoking the F-factor assumes that the supply of base cations from the watershed and atmospheric deposition to surface waters is a linear function of $SO_4^{2-} + NO_3^-$ concentrations which are derived from atmospheric deposition. To examine this assumption we plot simulated time series trajectories of ANC through hindcast simulations of (a), the sum of base cations (b) and soil percent base saturation (c) for three of the ALTM watersheds (Carry Pond, Arbutus Pond and Constable Pond (Fig. 10.6). The three sites were selected as examples to show a range of responses across the 20 ALTM lake watersheds simulated. The trajectories show a decrease in ANC (Fig. 10.6a) and an increase in C_B (Fig. 10.6b) with increasing concentrations of $SO_4^{2-} + NO_3^-$. After an initial period of relatively steady soil base saturation, soils acidify (i.e., loss of base saturation) with increases in concentrations of $SO_4^{2-} + NO_3^-$ (Fig. 10.6c). Following peak concentrations of $SO_4^{2-} + NO_3^-$, the lake watersheds show limited change in ANC with subsequent decreases in $SO_4^{2-} + NO_3^-$. There is a generally "linear-like" change in C_B with changes in $SO_4^{2-} + NO_3^-$; however, all lake watersheds show a hysteresis pattern where the waters have lower concentrations of C_B for a given concentration of $SO_4^{2-} + NO_3^-$ in the recovery leg of the trajectory, as compared with the acidification leg (Fig. 10.6b). Examining the slopes of change in C_B as a function of change in $SO_4^{2-} + NO_3^-$ ($\Delta C_B/C_A$; F-factor), this pattern is evident (Table 10.2). Initially, at the onset of acidic deposition, the F-factor is high due to the accelerated leaching of base cations from soil exchange sites. Over time, soil exchangeable base cations become depleted, the soil and water acidify in response to additional acidic deposition and F-factor values decrease. This loss of soil exchangeable base cation limits the recovery of ANC following decreases in acidic deposition.

Note that the three example lake watersheds have distinct patterns of ANC recovery. Carry Pond is increasing in ANC in response to decreases in lake $SO_4^{2-} + NO_3^-$ concentrations. Of the 20 ALTM lake watersheds simulated, 7 exhibit this type of recovery response. Arbutus Lake shows no change in ANC in response to decreases in lake $SO_4^{2-} + NO_3^-$ concentrations. Of the 20 ALTM lake watersheds simulated, 3 exhibit this type of recovery response. Finally Constable Pond is decreasing in ANC (continuing to acidify) in response to decreases in lake $SO_4^{2-} + NO_3^-$ concentrations. Of the 20 ALTM lake watersheds simulated, 10 are continuing to acidify under existing inputs of acidic deposition.

This analysis using PnET-BGC suggests that the assumption of a linear response of C_B to changes in $SO_4^{2-} + NO_3^-$, which is fundamental to many of the steady-state approaches to CLs for acidity, does not depict the dynamics of soil acid-base chemistry under changing acidic deposition. The non-linear behaviour of watershed base cation supply in response to changes in acidic deposition is a critical consideration in calculations of CLs for acidity. There are increasingly well-recognized uncertainties and limitations associated with the widely used simple steady-state CL modelling approaches for acidity (Curtis et al. 2001; Watmough et al. 2005). Such concerns have led to the more wide-spread use of process-based models that include the dynamics of base cation depletion in calculations of CLs for acidity (Rapp and Bishop 2009).

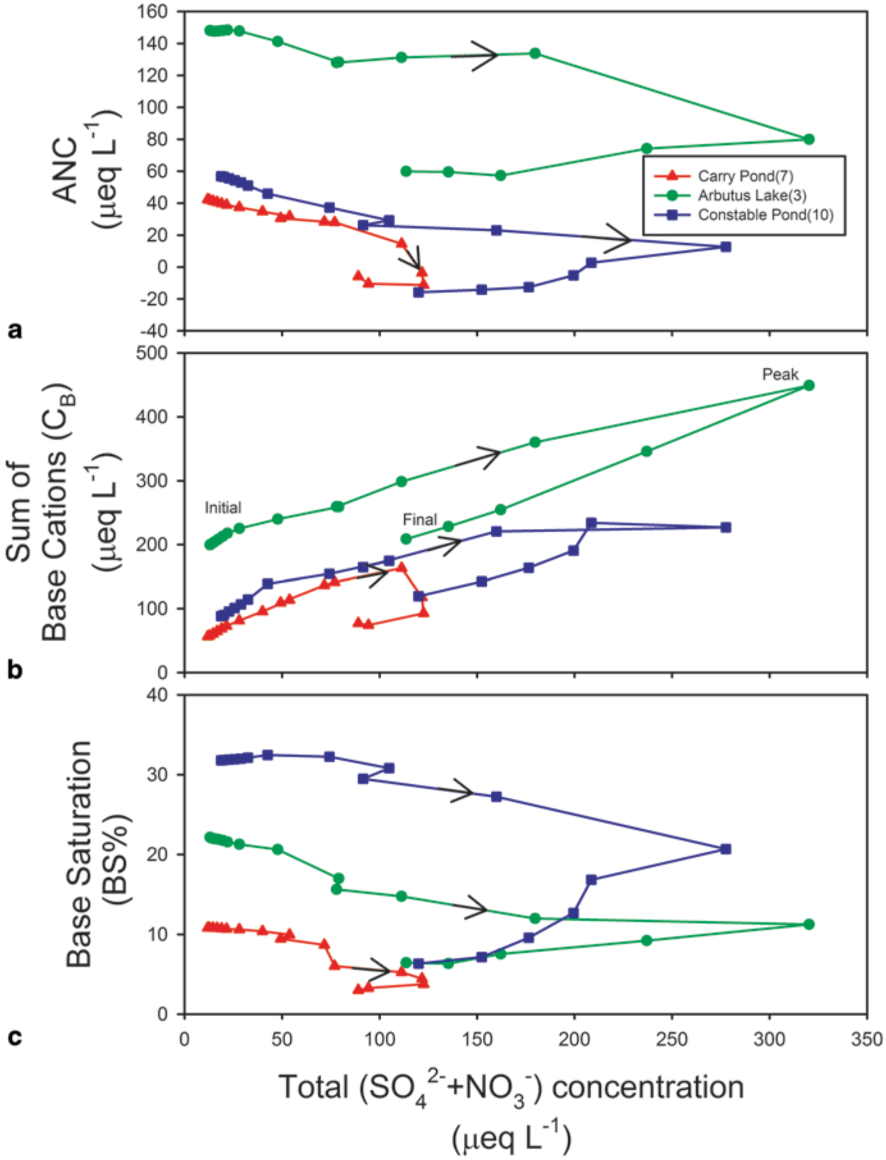

Fig. 10.6 Time series trajectories of PnET-BGC simulations of **a** acid neutralizing capacity (ANC); **b**, the sum of base cations (C_B), and **c** soil percent base saturation as a function of sulfate (SO_4^{2-}) plus nitrate (NO_3^-) concentrations for three Adirondack Long Term Monitoring (ALTM) watersheds (Carry Pond, Arbutus Pond and Constable Pond). Numbers in parenthesis refer to the number of 20 ALTM lakes simulated that show increases in ANC in response to decreases in acidic deposition (*7*); no change in ANC in response to decreases in acidic deposition (*3*); and further decreases in ANC in response to decreases in acidic deposition (*10*)

Table 10.2 Slopes of segments of time series of simulated hindcasts of the ratio of the change in sum of base cations to the change in the concentrations of sulfate plus nitrate ($\Delta C_B/\Delta C_A$: F-factor) for three Adirondack Long-Term Monitoring Lakes (see Fig. 10.6b)

ALTM lake	Carry pond	Arbutus lake	Constable pond
Initial slope (eq/eq)	1.74	2.06	1.88
Slope at peak C_A (eq/eq)	0.66	0.98	0.82
Slope at end of time series of C_A hindcast (eq/eq) (current conditions)	0.53	0.96	0.78

Discussion and Conclusions

The case studies included in this chapter illustrate the value of the combined approach for assessing CLs of N. Empirical CLs are needed to document ecosystem responses to N deposition under ambient conditions and as a reality check for simulation models. Biogeochemical models, on the other hand, provide the capability of evaluating ecosystem responses, including temporal dynamics, and CL exceedances under a variety of scenarios. Models can suggest how long it may take to reach various states of restoration. Models can also predict how climate change, disturbance, and land use scenarios will affect the CL. For example, DayCent simulations were used to evaluate the effectiveness of various combinations of decreased N deposition and prescribed fire intervals in reducing the impacts of excess N accumulation in forests of southern California (Gimeno et al. 2009).

Another advantage of biogeochemical models is that CLs can be estimated for a variety of ecological processes, pools or parameters. For example, CLs can be determined for acidification of soils or surface waters, NO_3^- leaching, stimulation of nitrification, nitrogenous trace gas emissions, biomass accumulation, or any other ecological parameter or process of interest that a model can effectively simulate. The ForSAFE-VEG model can estimate N CLs to protect plant biodiversity (Sverdrup et al. 2012).

Simulation models allow for hindcasting, forecasting, and the capability to evaluate a much wider combination of factors and environmental conditions than can be accomplished with empirical data or manipulative experiments. However, this can be an iterative process in that until further development, models may lack sufficient capability to effectively simulate the effects of some environmental factors that may influence the CL. Ecosystems are affected by multiple biotic and abiotic stressors which may include more than one type of pollutant, changing land use, or management approaches, in addition to a changing climate. Thus, empirical CLs determined from spatial gradient studies, N addition experiments, or long-term studies at one or a few sites may provide insights and CL estimates under multiple stress conditions with greater confidence than present models can provide. For example, in California mixed conifer forests, the CL for NO_3^- leaching or for effects on fine root biomass (Fenn et al. 2008) are likely affected by O_3 exposure; N deposition, including the changing ratio of reduced to oxidized N; fire suppression; and drought stress. Current models generally lack the functionality to estimate the CL as affected by these multiple co-occurring stressors. Thus, empirical CLs based on field observations may provide the best estimates of the N CL under these conditions. This points to the need of continuing model development for understanding these complex interactions and their implications for CLs and ecosystem protection.

Acknowledgments This research was funded in part by a National Science Foundation (USA) grant (NSF DEB 04–21530) and by New York State Energy Research and Development Authority.

References

Aber, J. D., Ollinger, S. V., & Driscoll, C. T. (1997). Modelling nitrogen saturation in forest ecosystems in response to land use and atmospheric deposition. *Ecological Modelling, 101,* 61–78.

Aber, J. D., Goodale, C. L., Ollinger, S. V., Smith, M.-L., Magill, A. H., Martin, M. E., Hallett, R. A., & Stoddard, J. L. (2003). Is nitrogen deposition altering the nitrogen status of Northeastern forests? *Bioscience, 53,* 375–389.

Allen, E. B., Rao, L. E., Steers, R. J., Bytnerowicz, A., & Fenn, M. E. (2009). Impacts of atmospheric nitrogen deposition on vegetation and soils in Joshua Tree National Park. In R. H. Webb, L. F. Fenstermaker, J. S. Heaton, D. L. Hughson, E. V. McDonald, D. M. Miller (Eds.), *The Mojave desert: Ecosystem processes and sustainability* (pp. 78–100). Las Vegas: University of Nevada Press.

Anderson, H. E. (1982). *Aids to determining fuel models for estimating fire behavior.* (General Technical Report INT-122). Ogden, Utah: USDA Forest Service Intermountain Forest and Range Experiment Station.

Baron, J. S. (2006). Hindcasting nitrogen deposition to determine an ecological critical load. *Ecological Applications, 16,* 433–439.

Baron, J. S., Ojima, D. S., Holland, E. A., Parton, W. J. (1994). Analysis of nitrogen saturation potential in Rocky Mountain tundra and forest: Implications for aquatic systems. *Biogeochemistry, 27,* 61–82.

Baron, J. S., Driscoll, C. T., Stoddard, J. L., & River, E. E. (2011a). Empirical critical loads of atmospheric nitrogen deposition for nutrient enrichment and acidification of sensitive US Lakes. *Bioscience, 61,* 602–613.

Baron, J. S., Driscoll, C. T., Stoddard, J. L. (2011b). Inland surface waters. In L. H. Pardo, M. J. Robin-Abbott, & C. T. Driscoll (Eds.), *Assessment of N deposition effects and empirical critical loads of nitrogen for ecoregions of the United States. General technical report NRS-80* (pp. 209–228). Newtown Square: U.S. Department of Agriculture, Forest Service, Northern Research Station.

Bergström, A.-K., & Jannson, M. (2006). Atmospheric nitrogen deposition has caused nitrogen enrichment and eutrophication of lakes in the northern hemisphere. *Global Change Biology, 12,* 635–643.

Bowman, W. D., Gatner, J. R., Holland, K., Wiedermann, M. (2006). Nitrogen critical loads for alpine vegetation and terrestrial ecosystem response: Are we there yet? *Ecological Applications, 16,* 1183–1193.

Brooks, M. L., & Minnich, R. A. (2006). Southeastern deserts bioregion. In N. G. Sugihara, J. W .V. Wagtendonk, K. E. Shaffer, J. Fites-Kaufman, & A. E. Thode (Eds.), *Fire in California's ecosystems* (pp. 391–414). Berkeley: University of California Press.

Brooks, M. L., D'Antonio, C. M., Richardson, D. M., Grace, J. B., Keeley, J. E., DiTomaso, J. M., Hobbs, R. J., Pellant, M., Pyke, D. (2004). Effects of invasive alien plants on fire regimes. *Bioscience, 54,* 677–688.

Brown, D. E., & Minnich, R. A. (1986). Fire and changes in creosote bush scrub of the western Sonoran desert, California. *American Midland Naturalist, 116,* 411–422.

Chen, L., & Driscoll, C. T. (2004). An evaluation of processes regulating spatial and temporal patterns in lake sulfate in the Adirondack region of New York. *Global Biogeochemical Cycles, 18,* GB3024, doi:10.1029/2003GB002169.

Chen, L., & Driscoll, C. T. (2005). Regional assessment of the response of the acid-base status of lake watersheds in the Adirondack region of New York to changes in atmospheric deposition using PnET-BGC. *Environmental Science & Technology, 39,* 787–794.

Curtis, C. J., Reynolds, B., Allott, T. E. H., Harriman, R. (2001). The link between the exceedance of acidity critical loads for freshwaters, current chemical status and biological damage: A re-interpretation. *Water, Air & Soil Pollution: Focus, 1,* 399–413.

De Vries, W., Kros, J., Reinds, G. J., Wamelink, G. W. W., Mol, J., van Dobben, H., Bobbink, R., Emmett, B., Smart, S., Evans, C., Schlutow, A., Kraft, P., Belyazid, S., Sverdrup, H. U., van Hinsberg, A., Posch, M., Hettelingh, J.-P. (2007). Developments in deriving critical limits and modelling critical loads of nitrogen for terrestrial ecosystems in Europe. (Report 1382). Wageningen, the Netherlands: Alterra Wageningen UR.

DeFalco, L. A., Bryla, D. R., Smith-Longozo, V., & Nowak, R. S. (2003). Are Mojave Desert annual species equal? Resource acquisition and allocation for the invasive grass *Bromus madritensis* subsp rubens (Poaceae) and two native species. *American Journal of Botany, 90,* 1045–1053.

Del Grosso, S. J., Parton, W. J., Mosier, A. R., Ojima, D. S., Kulmala, A. E., & Phongpan, S. (2000). General model for N_2O and N_2 gas emissions from soils due to denitrification. *Global Biogeochemical Cycles, 14,* 1045–1060.

Driscoll, C. T., Newton, R. M., Gubala, C. P., Baker, J. P., & Christensen, S. W. (1991). Adirondack mountains. In D. F. Charles (Ed.). *Acidic deposition and aquatic ecosystems: Regional case studies* (pp. 133–202). New York: Springer-Verlag.

Driscoll, C. T., Lawrence, G. B., Bulger, A. J., Butler, T. J., Cronan, C. S., Eagar, C., Lambert, K. F., Likens, G. E., Stoddard, J. L., & Weathers, K. C. (2001). Acidic deposition in the northeastern United States: Sources and inputs, ecosystem effects, and management strategies. *Bioscience, 51,* 180–198.

Driscoll, C. T., Driscoll, K. M., Roy, K. M., & Mitchell, M. J. (2003). Chemical response of lakes in the Adirondack region of New York to declines in acidic deposition. *Environmental Science & Technology, 37,* 2036–2042.

Elser, J. J., Andersen, T., Baron, J. S., Bergström, A. K., Jansson, M., Kyle, M., Nydick, K. R., Steger, L., Hessen, D. O. (2009). Shifts in lake N:P stoichiometry and nutrient limitation driven by atmospheric nitrogen deposition. *Science, 326,* 835.

Fenn, M. E., & Poth, M. A. (1999). Temporal and spatial trends in streamwater nitrate concentrations in the San Bernardino Mountains, southern California. *Journal of Environmental Quality, 28,* 822–836.

Fenn, M. E., Haeuber, R., Tonnesen, G. S., Baron, J. S., Grossman-Clarke, S., Hope, D., Jaffe, D. A., Copeland, S., Geiser, L., Rueth, H. M., Sickman, J. O. (2003). Nitrogen emissions, deposition, and monitoring in the western United States. *Bioscience, 53,* 391–403.

Fenn, M. E., Jovan, S., Yuan, F., Geiser, L., Meixner, T., Gimeno, B. S. (2008). Empirical and simulated critical loads for nitrogen deposition in California mixed conifer forests. *Environmental Pollution, 155,* 492–511.

Fenn, M. E., Sickman, J. O., Bytnerowicz, A., Clow, D. W., Molotch, N. P., Pleim, J. E., Tonnesen, G. S., Weathers, K. C., Padgett, P. E., Campbell., D. H. (2009). Methods for measuring atmospheric nitrogen deposition inputs in arid and montane ecosystems of western North America. In A. H. Legge (Ed.), *Developments in environmental science, Vol. 9: Air quality and ecological impacts: Relating sources to effects* (pp. 179–228). Amsterdam: Elsevier.

Fenn, M. E., Lambert, K. F., Blett, T. F., Burns, D. A., Pardo, L. H., Lovett, G. M., Haeuber, R. A., Evers, D. C., Driscoll, C. T., & Jeffries, D. S. (2011). *Setting limits: Using air pollution thresholds to protect and restore U.S. ecosystems*. (Issues in Ecology, Report Number 14). Washington: Ecological Society of America.

Gasche, R., Papen, H. (2002). Spatial variability of NO and NO_2 flux rates from soil of spruce and beech forest ecosystems. *Plant Soil, 240,* 67–76.

Gbondo-Tugbawa, S. S., Driscoll, C. T., Aber, J. D., & Likens, G. E. (2001). Evaluation of an integrated biogeochemical model (PnET-BGC) at a northern hardwood forest ecosystem. *Water Resources Research, 37,* 1057–1070.

Gimeno, B. S., Yuan, F., Fenn, M. E., Meixner, T. (2009). Management options for mitigating nitrogen (N) losses from N saturated mixed conifer forests in California. In A. Bytnerowicz, M. J. Arbaugh, A. R. Riebau, & C. Andersen (Eds.), *Wildland fires and air pollution. Developments in environmental science* (Vol. 8, pp. 425–455). Amsterdam: Elsevier.

Gundersen, P., Schmidt, I. K., & Raulund-Rasmussen, K. (2006). Leaching of nitrate from temperate forests—effects of air pollution and forest management. *Environmental Reviews, 14,* 1–57.

Hartman, M. D., Baron, J. S., Ojima, D. S. (2007). Application of a coupled ecosystem-chemical equilibrium model, DayCent-Chem, to stream and soil chemistry in a Rocky Mountain watershed. *Ecological Modelling, 200,* 493–510.

Hartman, M. D., Baron, J. S., Clow, D. W., Creed, I. F., Driscoll, C. T., Ewing, H. A., Haines, B. D., Knoepp, J., Lajtha, K., Ojima, D. S., Parton, W. J., Renfro, J., Robinson, R. B., van Miegroet, H., Weathers, K. C., Williams, M. W. (2009). *DayCent-Chem simulations of ecological and biogeochemical processes of eight mountain ecosystems in the United States.* (Report 2009–5150). U.S. Geological Survey Scientific Investigations.

Hettelingh, J. P., Posch, M., Slootweg, J. (2008). *Critical load, dynamic modelling and impact assessment in Europe. CCE status report 2008.* (RIVM Report 500090003). Bilthoven, The Netherlands: Coordination Centre for Effects, National Institute for Public Health and the Environment.

Interlandi, S. J., & Kilham, S. S. (2001). Limiting resources and the regulation of diversity in phytoplankton communities. *Ecology, 82,* 1270–1282.

Ito, M., Mitchell, M. J., & Driscoll, C. T. (2002). Spatial patterns of precipitation quantity and chemistry and air temperature in the Adirondack region of New York. *Atmospheric Environment, 36,* 1051–1062.

Kretser, W. J., Gallagher, J., & Nicolette, J. (1989). *Adirondack lake survey, 1984–1987: An evaluation of fish communities and water chemistry.* Ray Brook: Adirondack Lakes Survey Corporation.

Pardo, L. H., Fenn, M. E., Goodale, C. L., Geiser, L. H., Driscoll, C. T., Allen, E. B., Baron, J. S., Bobbink, R., Bowman, W. D., Clark, C. M., Emmett, B., Gilliam, F. S., Greaver, T. L., Hall, S. J., Lilleskov, E. A., Liu, L., Lynch, J. A., Nadelhoffer, K. J., Perakis, S. S., Robin-Abbott, M. J., Stoddard, J. L., Weather, K. C., & Dennis, R. L. (2011). Effects of nitrogen deposition and empirical nitrogen critical loads for ecoregions of the United States. *Ecological Application, 21,* 3049–3082.

Parton, W. J., Scurlock, J. M. O., Ojima, D. S., Gilmanov, T. G., Scholes, R. J., Schimel, D. S., Kirchner, T., Menaut, J. C., Seastedt, T., Moya, E. G., Kamnalrut, A., & Kinyamario, J. I. (1993). Observations and modeling of biomass and soil organic-matter dynamics for the grassland biome worldwide. *Global Biogeochemical Cycles, 7,* 785–809.

Parton, W. J., Hartman, M., Ojima, D., Schimel, D. (1998). DAYCENT and its land surface submodel: Description and testing. *Global Planet Change, 19,* 35–48.

Parton, W. J., Holland, E. A., Del Grosso, S. J., Hartman, M. D., Martin, R. E., Mosier, A. R., Ojima, D. S., & Schimel, D. S. (2001). Generalized model for NO_x and N_2O emissions from soils. *Journal of Geophysical Research: Atmospheres, 106,* 17403–17419.

Rao, L. E., & Allen, E. B. (2010). Combined effects of precipitation and nitrogen deposition on native and invasive winter annual production in California deserts. *Oecologia, 62,* 1035–1046.

Rao, L. E., Allen, E. B., & Meixner, T. (2010). Risk-based determination of critical nitrogen deposition loads for fire spread in southern California deserts. *Ecological Application, 20,* 1320–1335.

Rapp, L., & Bishop, K. (2009). Surface water acidification and critical loads: Exploring the F-factor. *Hydrology & Earth System Sciences, 13,* 2191–2201.

Riggan, P. J., Lockwood, R. N., & Lopez, E. N. (1985). Deposition and processing of airborne nitrogen pollutants in Mediterranean-type ecosystems of southern California. *Environmental Science & Technology, 19,* 781–789.

Saros, J. E., Clow, D. W., Blett, T., & Wolfe, A. P. (2011). Critical nitrogen deposition loads in high-elevation lakes of the western US inferred from paleolimnological records. *Water, Air & Soil Pollution, 216,* 193–202.

Skiba, U., Pitcairn, C., Sheppard, L., Kennedy, V., & Fowler, D. (2004). The influence of atmospheric N deposition on nitrous oxide and nitric oxide fluxes and soil ammonium and nitrate concentrations. *Water, Air & Soil Pollution: Focus, 4,* 37–43.

Smil, V. (2001). *Fritz Haber, Carl Bosch and the transformation of world food production*. Cambridge: The MIT Press.

Steers, R. J., & Allen, E. B. (2010). Post-fire control of invasive plants promotes native recovery in a burned desert shrubland. *Restoration Ecology, 18,* 334–343.

Sullivan, T. J., Cosby, B. J., Tonnessen, K. A., & Clow, D. W. (2005). Surface water acidification responses and critical loads of sulfur and nitrogen deposition in Loch Vale watershed, Colorado. *Water Resources Research, 41,* W01021.

Sverdrup, H., McDonnell, T. C., Sullivan, T. J., Nihlgård, B., Belyazid, S., Rihm, B., Porter, E., Bowman, W. D., & Geiser, L. (2012). Testing the feasibility of using the ForSAFE-VEG model to map the critical load of nitrogen to protect plant biodiversity in the Rocky Mountains region, USA. *Water, Air & Soil Pollution, 223,* 371–387.

Tonnesen, G., Wang, Z., Omary, M., & Chien, C. J. (2007). *Assessment of Nitrogen Deposition: Modeling and Habitat Assessment.* (CEC-500–2005-032. http://www.energy.ca.gov/2006publications/CEC-500-2006-032/CEC-500-2006-032.PDF). California Energy Commission, PIER Energy-Related Environmental Research.

USEPA. (2009). *Risk and Exposure Assessment for Review of the Secondary National Ambient Air Quality Standards for Oxides of Nitrogen and Oxides of Sulfur.* EPA-452/P-09–004a.

Walvoord, M. A., Phillips, F. M., Stonestrom, D. A., Evans, R. D., Hartsough, P. C., Newman, B. D., & Striegl, R. G. (2003). A reservoir of nitrate beneath desert soils. *Science, 302,* 1021–1024.

Watmough, S. A., Aherne, J., & Dillon, P. (2005). Effect of declining lake base cation concentration on freshwater critical load calculations. *Environmental Science & Technology, 39,* 3255–3260.

Williams, M. W., & Tonnessen, K. A. (2000). Critical loads for inorganic nitrogen deposition in the Colorado Front Range, USA. *Ecological Application, 10,* 1648–1665.

Wolfe, A. P., van Gorp, A. C., & Baron, J. S. (2003). Recent ecological and biogeochemical changes in alpine lakes of Rocky Mountain National Park (Colorado, USA): A response to anthropogenic nitrogen deposition. *Geobiology, 1,* 153–168.

Zhai, J., Driscoll, C. T., Sullivan, T. J., & Cosby, B. J. (2008). Regional application of the PnET-BGC model to assess historical acidification of Adirondack lakes. *Water Resources Research, 44,* W01421.